

Optimal Target Identification via Adaptive Radar Transmission

David A. Garren, Michael K. Osborn, Anne C. Odom, J. Scott Goldstein
Science Applications International Corporation
4001 Fairfax Drive, Suite 675
Arlington, VA 22203-1303, USA
david.a.garren@saic.com

S. Unnikrishna Pillai
Polytechnic University
Six Metrotech Center
Brooklyn, NY 11201, USA
pillai@hora.poly.edu

Joseph R. Guerci
Defense Advanced Research Projects Agency
Special Projects Office
Arlington, VA 22203, USA
jguerci@darpa.mil

Abstract – This paper investigates the optimization of both single and full polarization radar transmission waveforms to maximize target identification discrimination. This theory is applied to the discrimination of the T-72 and M1 battle tanks based upon simulated target frequency response data. Significant performance improvement in identification is obtained using an optimized transmission waveform over that of a standard chirped pulse.

1 INTRODUCTION

A number of researchers [1, 2, 3, 4, 5, 6, 7] have considered the use of sophisticated pulse shaping techniques in order to maximize the radar energy reflected off of a non-point target. In particular, Grieve, Guerci, Pillai, Oh, and Youla, [1, 2, 3] have developed a general theory of optimized pulse shaping that maximizes the target SINR, including the effects of both generic colored noise and colored signal-dependent clutter. In addition, Guerci and Pillai [8, 9] developed the theory of optimized pulse shaping for single-channel target identification discrimination via the use of techniques that are similar to that used for detection. This paper extends this target discrimination analyses in permitting multiple-channels, colored noise, and non-zero colored clutter.

The present analysis applies the theory of optimized pulse shaping for target identification discrimination using two simulated surface targets: the T-72 and M1 main battle tanks. SAIC-Champaign [10] generated the full-polarization VHF-band radar signatures for a single elevation angle of 15° and the full spectrum 0° – 360° of aspect angles relative to the sensor. These VHF-band data were

generated using the Fast Illinois Solver Code (FISC) that applies a method-of-moments technique to provide high fidelity at relatively low radar frequencies. The specific VHF-band data generated by SAIC-Champaign cover frequencies between 225-375 MHz at an aspect interval of 2°.

2 OPTIMIZED SINGLE-POLARIZATION TARGET IDENTIFICATION

The derivation begins with the result that the maximization of the probability of correct classification between two target classes α and β is equivalent [12, 13] to the maximization of the square of the Mahalanobis distance

$$\eta^2 \equiv (\mathbf{y}_\alpha - \mathbf{y}_\beta)^H \mathbf{R}^{-1} (\mathbf{y}_\alpha - \mathbf{y}_\beta) \quad (1)$$

between the two target echoes. Here, $\mathbf{y}_\alpha = \mathbf{q}_\alpha \mathbf{f}$ and $\mathbf{y}_\beta = \mathbf{q}_\beta \mathbf{f}$ are real-valued vectors of length $2N - 1$ giving the temporal samples of the echoes from targets α and β , respectively. The real-valued vector $\mathbf{f} \equiv [f_0, f_1, \dots, f_{N-1}]^T$ gives the temporal samples of the transmission pulse. The real-valued matrices \mathbf{q}_α and \mathbf{q}_β are the convolution impulse responses for targets α and β , respectively, having the form

$$\mathbf{q} = \begin{pmatrix} q_0 & 0 & \dots & 0 \\ q_1 & q_0 & \dots & 0 \\ \vdots & \vdots & \ddots & \vdots \\ q_{N-1} & q_{N-2} & \dots & q_0 \\ 0 & q_{N-1} & \dots & q_1 \\ \vdots & \vdots & \ddots & \vdots \\ 0 & 0 & \dots & q_{N-1} \end{pmatrix}. \quad (2)$$

20020807 252

The $(2N - 1) \times (2N - 1)$ Hermitian-Toeplitz matrix

$$\mathbf{R} = \begin{pmatrix} r_0 & r_1 & \cdots & r_{2N-2} \\ r_1^* & r_0 & \cdots & r_{2N-3} \\ \vdots & \vdots & \ddots & \vdots \\ r_{2N-2}^* & r_{2N-3}^* & \cdots & r_0 \end{pmatrix} \quad (3)$$

is the temporal autocorrelation of the noise plus clutter, with matrix coefficients

$$r_\ell \equiv \frac{1}{2\pi} \int_{-\pi}^{\pi} \{G_n(\omega) + G_c(\omega)|F(\omega)|^2\} e^{j\ell\omega} d\omega. \quad (4)$$

Thus, η^2 can be expressed in the form

$$\eta^2 = \mathbf{f}^H \Omega \mathbf{f}, \quad (5)$$

with the matrix Ω defined by

$$\Omega \equiv (\mathbf{q}_\alpha - \mathbf{q}_\beta)^H \mathbf{R}^{-1} (\mathbf{q}_\alpha - \mathbf{q}_\beta). \quad (6)$$

For the case of zero clutter $G_c(\omega) = 0$, the minimax theorem implies that the maximization of η^2 is obtained when the transmission pulse vector \mathbf{f} is equal to the eigenvector of Ω corresponding to the largest eigenvalue.

For the case of non-zero clutter $G_c(\omega) \neq 0$, the autocorrelation matrix \mathbf{R} depends upon the power spectrum $|F(\omega)|^2$ of the transmission pulse vector \mathbf{f} via Eqs. (3) and (4), so that an iterative procedure similar to that used for optimized target detection [2] must be applied, as described below:

- 1) For the initialization $k = 0$, begin with any real causal temporal vector \mathbf{f}_0 of duration t_0 and energy E_0 .
- 2) Let $\mathbf{f}_k \leftrightarrow F_k(\omega)$ and find the corresponding temporal autocorrelation matrix \mathbf{R}_k using Eqs. (3) and (4).
- 3) Compute the Ω_k matrix using Eq. (6) in terms of the autocorrelation matrix \mathbf{R}_k and the target impulse response matrix \mathbf{q} .
- 4) Find the largest eigenvalue $\lambda_1^{(k)}$ and corresponding normalized eigenvector $\mathbf{v}_1^{(k)}$ of the Ω_k matrix.
- 5) Define the error at stage k by

$$\epsilon_k = \sqrt{2\sqrt{E_0}(\sqrt{E_0} - \mathbf{f}_k^H \mathbf{v}_1^{(k)})}, \quad (7)$$

and invoke the same update rule that is applied in Pillai and Guerci [2]

$$\mathbf{f}_{k+1} = \frac{\mathbf{f}_k + \epsilon_k \mathbf{v}_1^{(k)}}{\sqrt{\left(1 + \frac{\epsilon_k}{\sqrt{E_0}}\right)^2 - \left(\frac{\epsilon_k}{\sqrt{E_0}}\right)^3}}. \quad (8)$$

- 6) Let $\mathbf{f}_{k+1} \leftrightarrow F_{k+1}(\omega)$ and go back to Step 2 with k replaced by $k + 1$, and repeat until ϵ_k is sufficiently small. Then the optimized transmission vector is

$$\mathbf{f} = \lim_{k \rightarrow \infty} \mathbf{f}_k. \quad (9)$$

Figure 1 gives the improvement in the square of the Mahalanobis distance squared between the T-72 and the M1 at VHF-band resulting from the use of the optimized transmission pulse over that of a standard chirped pulse. This figure shows two values of the CNR: 0 and 10. The improvement in the square of the Mahalanobis distance degrades as the CNR level is increased, as occurs with the SINR improvement in the detection problem [2].

For the case of aspect uncertainty, it is necessary to compute the expected value of the square of the Mahalanobis distance, i.e.,

$$\overline{\eta^2} = \int d\theta \xi(\theta) \eta^2(\theta) = \int d\theta \xi(\theta) \mathbf{f}^H \Omega(\theta) \mathbf{f}, \quad (10)$$

with the density function $\xi(\theta)$ characterizing the *a priori* likelihood of the target aspect θ . The matrix $\Omega(\theta)$ now includes aspect dependence, i.e.,

$$\Omega(\theta) = (\mathbf{w}_\alpha(\theta) - \mathbf{w}_\beta(\theta))^H \mathbf{R}^{-1} (\mathbf{w}_\alpha(\theta) - \mathbf{w}_\beta(\theta)). \quad (11)$$

Inserting Eq. (11) into Eq. (10) implies that

$$\overline{\eta^2} = \mathbf{f}^H \overline{\Omega} \mathbf{f}. \quad (12)$$

can be expressed in terms of

$$\overline{\Omega} = \int d\theta \xi(\theta) \Omega(\theta). \quad (13)$$

Thus, optimization of the transmission waveform to maximize identification performance under conditions of aspect uncertainty involves the computation of the weighted average of $\Omega(\theta)$ matrices with respect to aspect. Furthermore, the iterative procedure described above for the case of non-zero clutter is modified only by the replacement of the Ω matrix by its weighted average $\overline{\Omega}$.

3 OPTIMIZED FULL-POLARIZATION TARGET IDENTIFICATION

This section describes the theory of optimal waveform transmission and reception in order to maximize the Mahalanobis distance between two target echoes for the case of a single full-polarization waveform, i.e., one containing both horizontal and vertical components. Consider the $2N$ -length real-valued transmission signal vector and corresponding frequency response vector

$$\mathbf{f} \equiv \begin{pmatrix} \mathbf{f}_h \\ \mathbf{f}_v \end{pmatrix} \leftrightarrow \mathbf{F} \equiv \begin{pmatrix} \mathbf{F}_h \\ \mathbf{F}_v \end{pmatrix}, \quad (14)$$

with \mathbf{f}_h , \mathbf{f}_v , \mathbf{F}_h and \mathbf{F}_v each containing N temporal samples. The subscripts h and v denote the horizontal and vertical channels, respectively. This transmit vector is further constrained to have finite energy E_0 . This energy constraint corresponds to the case in which the sum of the transmission energies in both the horizontal and vertical channels are fixed, so that a single power supply supports both transmission channels. The $2N \times 2N$ target impulse response matrix and corresponding frequency response matrix have the form

$$\mathbf{q} = \begin{pmatrix} \mathbf{q}_{hh} & \mathbf{q}_{hv} \\ \mathbf{q}_{vh} & \mathbf{q}_{vv} \end{pmatrix} \leftrightarrow \mathbf{Q} \equiv \begin{pmatrix} \mathbf{Q}_{hh} & \mathbf{Q}_{hv} \\ \mathbf{Q}_{vh} & \mathbf{Q}_{vv} \end{pmatrix}. \quad (15)$$

The target echo vector has the form

$$\mathbf{s} \equiv \begin{pmatrix} s_h \\ s_v \end{pmatrix} = \mathbf{q}\mathbf{f}. \quad (16)$$

The full-polarization matrix

$$\mathbf{R} = \begin{pmatrix} \mathbf{r}_0 & \mathbf{r}_1 & \cdots & \mathbf{r}_{N-1} \\ \mathbf{r}_1^* & \mathbf{r}_0 & \cdots & \mathbf{r}_{N-2} \\ \vdots & \vdots & \ddots & \vdots \\ \mathbf{r}_{N-1}^* & \mathbf{r}_{N-2}^* & \cdots & \mathbf{r}_0 \end{pmatrix} \quad (17)$$

is the temporal autocorrelation of the noise plus clutter, with the 2×2 sub-matrix coefficients

$$\mathbf{r}_\ell \equiv \frac{1}{2\pi} \int_{-\pi}^{\pi} \{ \mathbf{G}_n(\omega) + \mathbf{G}_F(\omega) \} e^{j\ell\omega} d\omega. \quad (18)$$

The matrices $\mathbf{G}_n(\omega)$ and $\mathbf{G}_F(\omega)$ are the full-polarization spectral densities corresponding to the noise and the clutter, respectively. The total clutter power spectral density has the form

$$\mathbf{G}_F(\omega) \equiv \mathbf{G}_{hh}(\omega)|F_h(\omega)|^2 + \mathbf{G}_{hv}(\omega)F_h(\omega)F_v^*(\omega) \quad (19)$$

$$+ \mathbf{G}_{vh}(\omega)F_v(\omega)F_h^*(\omega) + \mathbf{G}_{vv}(\omega)|F_v(\omega)|^2 > 0 \quad (20)$$

The optimization of the transmission vector \mathbf{f} in order to maximize the square of the full-polarization Mahalanobis distance gives

$$\eta^2 = \max_{\mathbf{f}} \mathbf{f}^H \mathbf{\Omega} \mathbf{f}. \quad (21)$$

with the matrix $\mathbf{\Omega}$ defined by

$$\mathbf{\Omega} \equiv \{ \mathbf{q}_\alpha - \mathbf{q}_\beta \}^H \mathbf{R}^{-1} \{ \mathbf{q}_\alpha - \mathbf{q}_\beta \}. \quad (22)$$

For the case of zero clutter $\mathbf{G}_c(\omega) = 0$, the minimax theorem implies that the maximization of η^2 is obtained when the transmission pulse vector \mathbf{f} is equal to the eigenvector of $\mathbf{\Omega}$ corresponding to the largest eigenvalue. For the case of non-zero clutter $\mathbf{G}_c(\omega) \neq 0$, the autocorrelation matrix \mathbf{R} depends upon the full-polarization power spectrum of the transmission pulse vector \mathbf{f} via Eq. (20), so that the iterative

procedure described for single-polarization above must be applied.

Figure 2 gives the full-polarization waveforms optimized to maximize the Mahalanobis distance between the T-72 and the M1, as a function of the relative aspect angle for the case of white noise and zero clutter. The optimized waveform typically focuses the majority of its energy into a narrow frequency band corresponding to the maximum target response at that aspect angle. Figure 3 demonstrates that the optimized full-polarization waveform gives an improvement of 1-5 dB in the Mahalanobis distance over that obtained from the transmission of a full-polarization chirped waveform.

The analysis described above for the case of aspect certainty can be extended to the case of aspect uncertainty in a manner similar to that performed for the single-polarization case. The resulting theory requires a weighted-average with respect to relative aspect angle be performed on the autocorrelation kernel matrix $\mathbf{\Omega}$. This averaging of the full-polarization kernel matrices yields a smoothing of the Mahalanobis curves, as was obtained in the single-polarization case.

4 CONCLUSION

This study investigates the optimization of a single transmission pulse shape and the receiver impulse response in order to maximize the probability of correct identification between two target classes. The optimization of the transmission pulse shaping in order to maximize target identification performance that was developed by Guerri and Pillai [9] is extended to include multiple channels, colored noise, and non-zero colored clutter. These extensions [11] for the identification problem are developed via a maximization of the Mahalanobis distance, and thus the probability of correct classification, between the echoes of two target classes.

This study applies this theory [9] and extensions of optimized transmission pulse shaping in order to investigate the maximization of the probability of correct identification. Algorithmic implementation for the simulated T-72 and M1 frequency response data at both single and multiple polarizations of the VHF frequency band reveals significant improvements in the Mahalanobis distance of using a single optimized waveform over that of a standard chirped pulse.

5 ACKNOWLEDGMENTS

The authors gratefully acknowledge the assistance of Dennis J. Andersh and John T. Moore of SAIC-Champaign in providing the VHF-band and X-band frequency response data of the T-72 and M1 main battle tanks. In addition, the authors would like to thank Iram Weinstein, Jeffrey Wilcox,

Steven Huang, Matthew Weippert, and Chee-Yee Chong for useful suggestions.

References

- [1] P. G. Grieve and J. R. Guerci, "Optimum Matched Illumination-Reception Radar," U.S. Patent S517552, Filed: 18 June 1991, Issued: 29 December 1992.
- [2] S. U. Pillai, H. S. Oh, D. C. Youla, and J. R. Guerci, "Optimum Transmit-Receiver Design in the Presence of Signal-Dependent Interference and Channel Noise," *IEEE Transactions on Information Theory*, Vol. 46, No. 2, March 2000.
- [3] S. U. Pillai, H. S. Oh, and J. R. Guerci, "Multichannel Matched Transmit-Receiver Design in Presence of Signal-Dependent Interference and Noise," *Proceedings of the First IEEE Sensor Array and Multichannel Signal Processing Workshop*, 16-17 March 2000, Cambridge, MA.
- [4] D. T. Gjessing, "Target Adaptive Matched Illumination Radar Principles and Applications," IEE Electromagnetic Waves Series (22), Peter Peregrinus Ltd., 1986.
- [5] A. Farina and F. A. Studer, "Detection with High Resolution Radar: Great Promise, Big Challenge," *Microwave Journal*, pp. 263-273, May 1991.
- [6] I. J. LaHaie, R. O. Harger, S. R. Robinson, J. K. Miller, "An Evaluation of Nonsinusoidal Radar Techniques," Final Report, AD-A171-484, ERIM, Ann Arbor, MI, June 1985.
- [7] H. H. Schrieber and M. G. O'Connor, "Adaptive Waveform Radar," U.S. Patent 4,901,082, February 1990.
- [8] J. R. Guerci, "Optimum Matched Illumination-Reception Radar for Target Classification," U.S. Patent S5381154, Filed: 3 September 1993, Issued: 10 January 1995.
- [9] J. R. Guerci, and S. Pillai, Unnikrishna, "Theory and Application of Optimum Transmit-Receive Radar," *Proceedings of the IEEE International Radar Conference*, 07-12 May 2000, Alexandria, VA, p. 705.
- [10] D. Andersh, J. Moore, S. Kosanovich, D. Kapp, R. Bhalla, R. Kipp, T. Courtney, A. Nolan, F. German, J. Cook, and J. Hughes, "XPatch4: The Next Generation in High Frequency Electromagnetic Modeling and Simulation Software," *IEEE 2000 International Radar Conference*, 07-12 May 2000, Alexandria, VA, pp. 844-9.
- [11] D. A. Garren, M. K. Osborn, A. C. Odom, J. S. Goldstein, S. U. Pillai, and J. R. Guerci, "Optimization of Single Transmit Pulse Shape to Maximize Detection and Identification of Ground Mobile Targets," to appear in *Proceedings of 34th Asilomar Conference on Signals, Systems, and Computers*, Pacific Grove, CA, 29 October - 01 November, 2000.
- [12] H. L. Van Trees, *Detection, Estimation, and Modulation Theory: Part I*, New York: Wiley, 1968.
- [13] C.-Y. Chong, private communication.

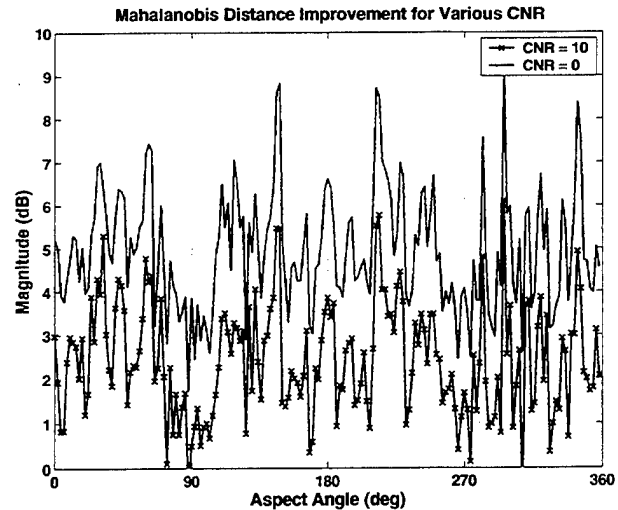


Figure 1. This plot presents the Mahalanobis distance improvement at VHF-band with respect to a chirped transmission waveform resulting from use of a transmission pulse shape optimized for T-72 versus M1 identification discrimination. The two curves corresponding to $\text{CNR} = 1$ and $\text{CNR} = 10$ are plotted as a function of aspect for $0^\circ - 360^\circ$.

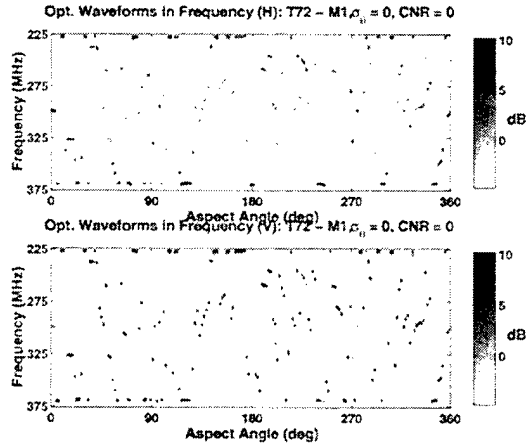


Figure 2. This figure gives the full-polarization waveforms optimized to maximize the Mahalanobis distance between the T-72 and the M1, as a function of the relative aspect angle for the case of white noise and zero clutter. The optimized waveform typically focuses the majority of its energy into a narrow frequency band corresponding to the maximum target response at that aspect angle.

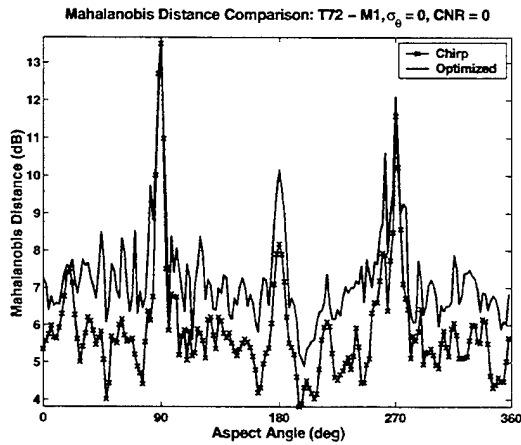


Figure 3. This figure demonstrates that the optimized full-polarization waveform gives an improvement of 1-5 dB in the Mahalanobis distance over that obtained from the transmission of a full-polarization chirped waveform.